Metastasis-associated Differences in Gene Expression in a Murine Model of Osteosarcoma

Chand Khanna,[1] Javed Khan, Phoungmai Nguyen, Jennifer Prehn, Jana Caylor, Choh Yeung, Jane Trepel, Paul Meltzer, and Lee Helman

Pediatric Oncology [C. K., J. P., J. C., C. Y., L. H.] and Medicine Branches [P. N., J. T.], National Cancer Institute, and Cancer Genetics Branch, Human Genome Research Institute, NIH [J. K., P. M.], Bethesda, Maryland 20892

ABSTRACT

Despite advances in the management of osteosarcoma (OSA) and other solid tumors, the development of metastasis continues to be the most significant problem and cause of death for cancer patients. To define genetic determinants of pulmonary metastasis, we have applied cDNA microarrays to a recently described murine model of OSA that is characterized by orthotopic tumor growth, a period of minimal residual disease, spontaneous pulmonary metastasis, and cell line variants that differ in metastatic potential. Microarray analysis defined 53 genes (of 3166 unique cDNAs) that were differentially expressed between the primary tumors of the more aggressive (K7M2) and less aggressive (K12) OSA models. By review of the literature, these differentially expressed genes were assigned to six nonmutually exclusive metastasis-associated categories (proliferation and apoptosis, motility and cytoskeleton, invasion, immune surveillance, adherence, and angiogenesis). Functional studies to evaluate K7M2 and K12 for differences in each of these metastasis-associated processes revealed enhanced motility, adherence, and angiogenesis in the more aggressive K7M2 model. For this reason, 10 of the 53 differentially expressed genes that were assigned to the motility and cytoskeleton, adherence, and angiogenesis categories were considered as most likely to define differences in the metastatic behavior of the two models. *Ezrin,* a gene not described previously in OSA, with functions in motility, invasion, and adherence, was 3-fold overexpressed in K7M2 compared with K12 by microarray. Differential expression for RNA was confirmed by Northern analysis and for protein by immunostaining. Alterations in ezrin protein levels and concomitant cytoskeletal changes in our model confirmed predictions from the arrays. The potential relevance of ezrin in OSA was suggested by its expression in five of five human OSA cell lines. This work represents a rationale approach to the evaluation of microarray data and will be useful to identify genes that may be causally associated with metastasis.

INTRODUCTION

OSA[2] is the most common primary tumor of bone. Similar to other solid tumors, it is characterized by a high propensity for metastasis (*i.e.,* the lungs, liver, and bone). In OSA, the lung is the most common site for metastasis. In spite of successful control of the primary tumor, death from pulmonary metastases occurs in >30% of patients within 5 years (1). A greater understanding of the biology of pulmonary metastases is needed to improve treatment outcomes and identify patients with the highest risk for disease relapse in OSA and other solid tumors. We have described recently a relevant murine model of OSA characterized by tumor growth at appendicular sites (orthotopic), a period of minimal residual disease, spontaneous pulmonary metastasis, and model variants that differ in metastatic potential (2). This model was developed from a cell line (K12) originating from a spontaneous BALB/c OSA (3) and a recently derived, clonally related

cell line (K7M2) described by the authors (2). Within the model, the K7M2 cell line is aggressive and highly metastatic, whereas the K12 cell line is less aggressive with infrequent pulmonary metastases (Fig. 1). In K7M2, spontaneous pulmonary metastases from an orthotopic primary tumor develop in >90% of mice compared with K12, where only 33% of mice develop metastases ($P < 0.001$).

The differences in metastatic potential of the clonally related cell lines characterized in this model make it a valuable system for understanding the biology of pulmonary metastases in OSA. Genetic risk factors for pulmonary metastasis have been defined in several solid tumors (4–6). The majority of this work has been undertaken in epithelial malignancies. Similar to other solid tumors, OSA metastases are associated with dissemination through the blood stream (hematogenous), microscopic metastasis (micrometastases) that exist in the absence of observable metastases, and a high propensity for metastases to the lung (7). Distinctive features of metastasis in OSA include an uncharacteristically long latency between successful control of the primary tumor and the development of pulmonary metastases, a preference for pulmonary metastases compared with other metastatic sites, and relative success associated with surgical removal of pulmonary metastases (1). The use of this nonepithelial model provides a unique perspective in the study of metastasis that may uncover novel determinants for metastasis relevant to both mesenchymal and epithelial cancers.

To define genetic determinants of metastasis in OSA, we have used cDNA microarrays to compare gene expression between the clonally related high metastatic (K7M2) and low metastatic (K12) primary tumors. Array comparisons of K7M2 and K12 have defined 53 of 3166 unique printed cDNA probes (genes) that are differentially expressed. To focus our attention on a smaller group of potentially important genes, we have taken a functional approach to determine the significance and relevance of these differentially expressed genes vis à vis pulmonary metastasis. By review of the literature, we have assigned each differentially expressed gene to six nonmutually exclusive metastasis-associated categories including proliferation and apoptosis, motility and cytoskeleton, invasion, immune surveillance, adherence, and angiogenesis (7). K7M2 and K12 were then compared in studies that independently examined each of these metastasis-associated processes. These studies (some presented in the initial description of the model; Ref. 2) demonstrated increased cellular motility and cytoskeletal changes suggestive of motile cells, earlier heterotypic adherence, and enhanced tumor angiogenesis in the more aggressive K7M2 compared with the less aggressive K12 model. On the basis of this functional and metastasis-related characterization, 10 genes that were assigned to the cell motility and cytoskeleton, heterotypic adherence, and angiogenesis categories were considered to be most likely to describe the aggressive behavior of K7M2 compared with the K12 cells. *Ezrin,* a member of the *ERM* gene family was 1 of these 10 genes. Similar to other members of its gene family, *ezrin* plays a role in linking the actin cytoskeleton to the cell membrane (8, 9). *Ezrin* has been associated with cell motility, invasion, and adherence but has not been described previously in OSA. Differential expression of *ezrin* between K7M2 and K12 was confirmed at both
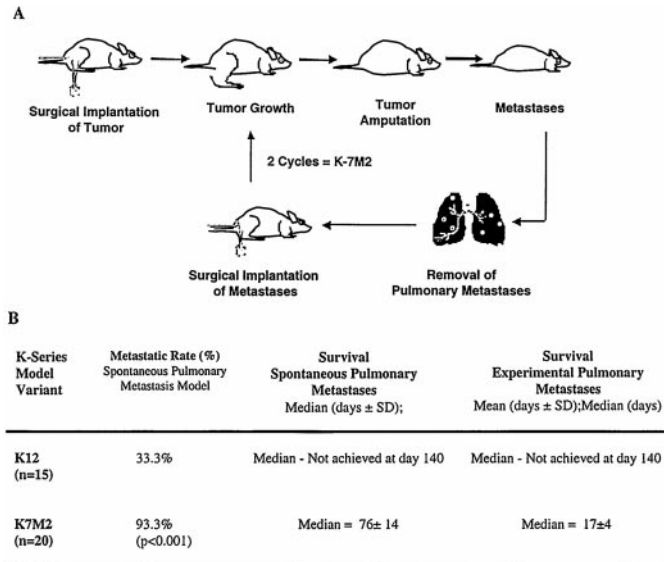
Fig. 1. Orthotopic tumor model used to characterize and derive the clonally related aggressive (*K7M2*) and less aggressive (*K12*) murine OSA cell lines. *A*, illustration of model design used to implement the model and to develop the more aggressive K7M2 clone from the less metastatic parent cell. *B*, characterization of differences in metastatic behavior of the more aggressive K7M2 model and less aggressive K12 model.

mRNA and protein levels. *In situ* differences in the distribution of ezrin protein suggested a role of ezrin in the motility of K7M2 cells. The relevance of ezrin in human OSA was supported by Northern analysis that demonstrated its expression in five of five human OSA cell lines.

MATERIALS AND METHODS

Animal Model. The K12 murine OSA cell line was a kind gift of L. C. Gerstenfeld (3, 10). K7M2 was derived within the presented model system (Fig. 1) by two cycles of pulmonary metastasis implantation to the proximal tibia. The model conditions and characterization of the highly metastatic cell line, K7M2, and less metastatic cell line, K12, are summarized in Fig. 1. K7M2 and K12 cells were maintained *in vitro* using complete culture media [DMEM; Celox Co., Hopkins, MN; 100 μg/ml penicillin-streptomycin; and 2 mM L-glutamine (Sigma Chemical Co., St. Louis, MO)] with 10% FCS (Sigma Chemical Co.) at 37°C at 5% CO_2. All cell lines used for *in vitro* and *in vivo* studies were from the 3rd to 15th passages. For all *in vitro* assays, cells were harvested, using Trypsin/Versene, from near-confluent cultures. Cell viability was assessed using trypan blue, and experiments were not continued if cell viability was <90%.

RNA Extraction. RNA was extracted from *in vitro* tumor cell lines using the Qiagen RNeasy Midi kit (Qiagen, Inc., Valencia, CA) according to the manufacturer's specification. RNA was extracted from grossly dissected primary tumor and from pulmonary metastases using the Trizol (Life Technologies, Inc., Rockville, MD) reagent according to the manufacturer's specification. Extracted RNA was quantitated by spectrophotometry and then examined by 1% agarose gel (Seakem GTG; FMC Bioproducts, Rockland, ME) electrophoresis. Intact RNA was then reextracted in 1.0 ml of Trizol for use in microarray experiments.

Microarrays, Probes, Hybridization, and Scanning. The mouse array is composed of 3899 detector elements (probes). Of these, 315 are unclustered ESTs, 630 are clustered ESTs, and 3004 are clustered, named genes. There is significant redundancy in the named gene portion of the set, with 2221 unique clusters (probes) represented. All clones (including clustered and unclustered ESTs) were obtained from Research Genetics (Huntsville, AL); selection of probes was based only on availability. Clustering was undertaken by Research Genetics. PCR products from these clones were prepared and printed onto glass slides according to protocols described previously (11, 12). Fluorescent cDNA targets (samples) were labeled with either Cy3 or Cy5 (Amersham Pharmacia Biotech, Piscataway, NJ) from 100 to 200 μg of total RNA by oligo

dT-primed polymerization using SuperScript II reverse transcriptase (Life Technologies, Inc., Rockville, MD) as described previously (11, 12). Imaging and image analysis was as described previously (11, 12). Normalization for differential efficiencies of labeling and detection was performed using all spots (probes) that performed well as defined by criteria embedded in the DeArray software developed by Chen *et al.* (13). The normalization constant from these genes was then used to calculate the calibrated ratio for every cDNA probe within the image. Furthermore, the ratio variation of the these genes determined the confidence interval in which ratios are to be considered as no difference from 1.0. The 99% confidence interval was used throughout the experiments to test the significance of differentially expressed genes. Additional information on the image analysis as well as the raw data including the hybridization images for each sample is available on the Internet.[3] Microarray outliers were defined as those genes that were significantly differentially expressed and that had a MaxMean signal intensity (defined as the maximum of the mean intensity of either the red or green channel for each gene) >2000 in two distinct array experiments (using samples from different mice bearing the K7M2 and K12 primary tumors). Differential expression of randomly selected genes was confirmed by Northern analysis. Northern blots consisted of 25 μg of total RNA from K7M2 and K12 cell lines, primary tumors, and pulmonary metastases. Plasmid probes, purified by MaxiPrep (Qiagen, Inc., Valencia, CA) containing sequence-confirmed cDNAs, were labeled by nick translation (Amersham, Life Science) with [α-^{32}P]dCTP. Hybridization of Northern blots was carried out using Express Hyb (Clontech, Palo Alto, CA), according to the manufacturer's recommendations. Equal loading of RNA was verified by reprobing all Northern blots with an [α-^{32}P]dCTP-labeled murine β-actin plasmid probe. Northern analysis for ezrin in human OSA cell lines (HOS, MG63, U2, G292, and SaOS) was undertaken using a nick-translated plasmid provided generously by Dr. Richard Lamb (8).

Assignment of Microarray Outliers to Protein Function and Metastasis-related Gene Process Categories. Differentially expressed genes, identified from cDNA microarray comparisons, were assigned to a modification of the NCBI Clusters of Orthologous Gene classification by searching the OMIM and PubMed databases by gene name.[4] Genes were then assigned to six nonmutually exclusive metastasis-associated processes (proliferation/apoptosis, motility/cytoskeleton, invasion, adhesion, immune surveillance, and angiogenesis) using a PubMed database search of the gene name and each of the following terms: cancer, metastasis, proliferation, apoptosis, invasion, motility, immune surveillance, adhesion, and angiogenesis. Each gene was categorized with a single and mutually exclusive function, whereas gene assignment to metastasis-associated processes was not mutually exclusive.

Actin Cytoskeleton. Cells were grown on sterile coverslips fixed with 3.7% formaldehyde in PBS for 10 min and then extracted with 0.2% Triton X-100 for 10 min at room temperature. After fixation and extraction, one unit of rhodamine phalloidin (Molecular Probes, Eugene, OR) was added to the coverslip prepared cells, as recommended by the manufacturer, and incubated at room temperature. After 1 h, the coverslip was washed two times for 2 min with PBS. Cells were stained with 0.4 μg/ml of 4′,6-diamidino-2-phenylindole (Sigma Chemical Co.) for 10 min at room temperature. After incubation, the coverslip was washed with PBS, rinsed quickly with water, air-dried, and mounted onto slides using SlowFade (Molecular Probes). Cells were visualized on a Zeiss Axiovert microscope using a ×63 objective, and images were captured with an Optronics CCD camera.

Motility and Invasion Assays. Preincubation of 12-mm polycarbonate Transwell (Costar, Cambridge MA) plates for 4 h at 37°C was undertaken by adding complete culture medium to the upper chamber and complete culture medium with 10% FCS to the lower chamber before the addition of cells. Five thousand K7M2 or K12 cells were added in a volume of 200 μl of serum-free complete medium to the upper Transwell chamber. The Transwell upper chamber was placed into lower chambers that had been filled with 500 μl of complete medium with 10% FCS. For the Matrigel (Collaborative Biomedical Products, Bedford. MA) invasion assay, 100 μl of a 1:3 dilution of Matrigel in serum-free culture medium was added to the upper chamber of the Transwell and incubated for 2 h at 37°C (after the preincubation step). Transwell plates (motility assay) and Transwell plates coated with Matrigel (invasion assay) were incubated for 4, 12, 24, and 48 h at 37°C. At the completion of the

---

[3] Internet address: http://www.nhgri.nih.gov/DIR/LCG/arraydb/.
[4] Internet address: http://www.ncbi.nlm.nih.gov/cgi-bin/COG/palog?fun=all.

Table 1 *Microarray (cDNA) outliers overexpressed in K7M2 primary tumors versus K12 primary tumors*

Gene name organized by designated gene function (modification of clusters of orthologous sites)[a]	IMAGE ID[b]	Mean[c]	Proliferation/Apoptosis	Motility/Cytoskeleton	Invasion	Immune surveillance	Adhesion	Angiogenesis
I. Information storage and processing								
Translation, ribosomal structure and biogenesis								
Protein kinase, interferon inducible double stranded RNA dependent	597390	3.11	●			●		
Transcription								
Glucocorticoid-induced leucine zipper (GILZ)	476319	5.82						
Myeloblastosis oncogene	577875	3.54	●					
CCAAT/enhancer binding protein (C/EBP), α	891375	2.84	●					
Caudal type homeo box 2	437757	2.70	●					
Hepatocyte nuclear factor 3/forkhead homologue 8	537201	2.55						
Nuclear factor, erythroid derived 2, ubiquitous	576400	2.39	●					
E2F-5	585020	2.29	●					
DNA replication, recombination, and repair								
Fibroblast inducible secreted protein (connective tissue growth factor)	598684	3.16	●					●
II. Cellular processes								
Cell division and chromosome partitioning								
Cyclin D1	419285	5.57	●		●			
Tubulin β-chain	467387	2.60	●	●				
Posttranslational mod., protein turnover, chaperones								
Proprotein convertase subtilisin/kexin type 3	334336	8.19						
α-Crystallin A chain-major component	481224	2.60						
mSTI1	614877	2.25						
Cell motility/cell and matrix interaction-communication								
Integrin β 4	337221	5.60	●	●	●		●	
Integrin α-V (CD51)	960079	3.64		●	●		●	●
Ezrin	635783	2.95	●	●	●		●	
Integrin β2	583119	2.84				●	●	
Galectin-3	571813	2.50	●	●	●		●	
A disintegrin and metalloprotease domain (ADAM) 8	582054	2.49		●	●		●	
Inorganic ion transport and metabolism								
Metallothionein 2	607350	2.48	●					
Signal transduction mechanisms								
ATP receptor (P2u)	405832	2.83	●					
III. Metabolism								
Protein/amino acid transport and metabolism								
Pyrroline-5-carboxylate synthetase short isoform	439868	3.49						
Asparagine synthetase	605295	3.23	●					
Lipid metabolism								
Clusterin	617298	2.59	●			●	●	
IV. Cell structure/matrix								
Extracellular matrix								
Myelin proteolipid protein	524747	3.05						
V. Poorly characterized								
A10	533608	7.70						
Major histocompatibility locus class III regions	420495	2.59						
VI. ESTs or Unknown Genes								
EST, not currently in a UniGene cluster	400844	3.63						
EST, not currently in a UniGene cluster	420591	3.60						
EST, not currently in a UniGene cluster	409208	2.49						

[a] Classification, using a modification of the NCBI Clusters of Orthologous Gene Classification, based on the basic function of each outlier gene.

[b] IMAGE clone identification for differentially expressed genes.

[c] Geometric mean of red:green ratios from two-array experiment. Colorimetric representation of geometric mean of red:green ratio with scale available online at www-dcs.nci.nih.gov/pedonc.

[d] Metastasis-related categories include proliferation and apoptosis, motility and cytoskeleton, invasion, immune surveillance, adherence, and angiogenesis. ●, assignment of genes to metastasis-related categories. Assignment of genes based on PubMed literature search.

incubation period, culture medium was suctioned from upper and lower chambers without disturbing cells. The total number of (motile or invasive) cells moving through the Transwell membrane was determined in replicates of six by wiping the apical surface of the Transwell membrane with a cotton swab and then staining the Transwell insert with DiffQuick (American Scientific Products, McGraw Park, IL). The Transwell membrane was then cut out using a No. 11 scalpel blade (Becton Dickinson Acute Care, Franklin Lakes, NJ), mounted, and coverslipped on a microscopic slide for cell enumeration. The total number of plated cells was evaluated at each time point (in replicates of six) by eliminating the "cotton swab step" and repeating the staining and membrane preparation procedure described above. The percentage of motility and percentage of invasion = (total number of cells on basilar surface of membrane)/(total number of cells on both apical and basilar surfaces of the membrane). Motility and invasion experiments were each repeated three times. Representative results from experimental conditions, repeated in replicates of six, are presented.

Gelatinase Zymography. Gelatinase zymography was used to evaluate MMP2 and MMP9 activity in tissue culture supernatant and primary tumor as described previously (14). Serum-free medium was placed on confluent cultures of K7M2 and K12 for 24 h. Protein content in culture supernatants was quantified using the bicinchoninic acid assay (Pierce, Rockford, IL). Up to 25 μg of total protein were evaluated by gelatin electrophoresis (Novex Gel; Invitrogen, Carlsbad, CA). Standards for the pro and active forms of MMP2 and MMP9 (Calbiochem, La Jolla, CA) allowed identification of MMP forms.

Heterotypic Adherence Assay. K7M2 and K12 cells were added to 96-well, flat-bottomed, substrate-coated plates (collagen type IV precoated plates

Table 2 *Microarray (cDNA) outliers overexpressed in K12 primary tumors versus K7M2 primary tumors*

Gene name organized by designated gene function (modification of clusters of orthologous sites)[a]	IMAGE ID[b]	Mean[c]	Proliferation/Apoptosis	Motility/Cytoskeleton	Invasion	Immune surveillance	Adhesion	Angiogenesis
I. Information storage and processing								
Transcription								
Stra13	596504	0.23	●					
Nephroblastoma overexpressed gene	475200	0.28	●					
DNA replication, recombination, and repair								
Bcl-2 α	596444	0.25	●					
II. Cellular processes								
Posttranslational mod., protein turnover, chaperones								
Apolipoprotein B editing complex 2	603777	0.33						
Regulatory protein, T lymphocyte 1	617776	0.37				●		
Cell motility/cell and matrix interaction-communication								
Decorin	598629	0.25	●		●			
FARP1	403430	0.35	●	●			●	
Inorganic ion transport and metabolism								
Ceruloplasmin	522108	0.25				●		●
Signal transduction mechanisms								
G-protein coupled receptor	574735	0.45		●				
III. Metabolism								
Energy production and conversion								
Carbonic anhydrase 3	618431	0.36						
Carbohydrate transport and metabolism								
Skeletal muscle calsequestrin	474650	0.32						
Lipid metabolism								
Mast cell protease 5	493561	0.36						
Lipoprotein lipase	475661	0.38						
IV. Cell structure/matrix								
Cell membrane								
Membrane metallo endopeptidase	313540	0.11	●					
Potassium voltage gated channel, Shaw-related subfamily, member 1	493098	0.31						
CD83	574651	0.37				●		
Cytoskeleton								
Ankyrin 1, erythroid	635047	0.36						
Extracellular matrix								
Secreted phosphoprotein 1 (Osteopontin)	337866	0.45						
V. Poorly characterized								
Selected mouse cDNA on the Y	598638	0.26						
Fibrinogen-like protein 2	336457	0.36						
Histidine-rich calcium-binding protein	475063	0.44						
VI. ESTs or unknown genes								
EST	522100	0.22						

[a] Classification, using a modification of the NCBI Clusters of Orthologous Gene Classification, based on the basic function of each outlier gene.

[b] IMAGE clone identification for differentially expressed genes.

[c] Geometric mean of red:green ratios from two-array experiment. Colorimetric representation of geometric mean of red:green ratio with scale available online at www-dcs.nci.nih.gov/pedonc.

[d] Metastasis-related categories include proliferation and apoptosis, motility and cytoskeleton, invasion, immune surveillance, adherence, and angiogenesis. ●, assignment of genes to metastasis-related categories. Assignment of genes based on PubMed literature search.

and Matrigel precoated plates; Becton Dickinson, Bedford, MA) in quadruplicate. Cells were incubated at 37°C in 5% CO_2 for 0.5, 1.5, 4, 16, 24, or 48 h. After incubation, medium was carefully suctioned out of each well. Using a multichannel pipette in a controlled manner, each well was washed three times with PBS (Biofluids, Inc., Rockville, MD). Between each wash, the plate was manually rocked back and forth three times. PBS was carefully suctioned out of each well. After the washes, the 3-(4,5-dimethylthiazol-2-yl)-2,5-diphenyltetrazolium bromide assay was used to determine the number of remaining cells (adherent cells; Ref. 15). The percentage of adherence for each time point = (mean number of cells remaining in a well after washing)/(mean number of cells in wells that were not washed).

Immune Surveillance. Female beige-scid mice (Charles River Laboratories, Wilmington, MA), 4–5 weeks of age, were housed under pathogen-free conditions with a 12-h light/12-h dark schedule and fed autoclaved standard chow and water *ad libitum. In vitro* passaged tumor cell lines (K7M2 and K12) were harvested and prepared for injection as described previously (16). Cells were brought to a final concentration of 1×10^7 cells/ml in phenol-free HBSS and kept at 4°C. Cells were enumerated, and viability was assessed using trypan blue (BioWhittaker, Walkersville, MD) staining. Experiments were continued if cell viability was >90%. A volume of 100 μl (1×10^6 cells) was injected into the lateral tail vein of beige-scid mice (10 mice/cell line). Mice

were monitored at least three times weekly for evidence of morbidity associated with pulmonary metastases. Criteria for morbidity associated with metastases in mice included ill thrift, anorexia, dehydration, decreased activity and grooming behavior, and dyspnea. Sacrifice of mice with presumed pulmonary metastases was primarily based on the development of dyspnea. All mice that were sacrificed because of presumed pulmonary metastases had necropsy confirmation of diffuse metastases. Statistical comparisons were made using the Kruskal-Wallace nonparametric *t* test calculated with InStat for the MacIntosh. Statistical significance was defined as $P < 0.05$. Animal care and use were in accordance with guidelines of the NIH Animal Care and Use Committee (17).

Ezrin Immunocytostaining. Coverslip preparations were fixed and extracted as described above. Nonspecific binding sites were blocked by incubating the cells with 1% BSA in PBS for 1 h at 4°C before processing for immunofluorescence labeling. Anti-ezrin antibody (Santa Cruz Biotechnology, Santa Cruz Biotechnology, CA) was added to the coverslip and incubated for 1 h at 4°C. After antibody incubation, the coverslip was washed two times for 2 min with PBS and incubated at 4°C with Cy3-conjugated rabbit antigoat immunoglobulin (Jackson Immunoresearch Laboratories, Inc). After 1 h, the coverslip was washed two times for 2 min with PBS. Cells were stained with 0.4 μg/ml of 4′,6-diamidino-2-phenylindole (Sigma Chemical Co.) for 10 min

at room temperature. The coverslip was then washed with PBS, rinsed quickly with water, air-dried, and mounted onto slides using SlowFade (Molecular Probes). Cells were visualized on a Zeiss Axiovert microscope using a ×63 objective, and images were captured with an Optronics CCD camera.

RESULTS

cDNA Microarray Analysis. Microarray experiments examined differences in gene expression between the primary tumors of the more aggressive K7M2 and less aggressive K12 models. Fifty-three cDNAs of 3166 were found to be differentially expressed (expression ratios not equal to 1.0 with 99% confidence; MaxMean signal intensity, >2000) in replicate microarray experiments using primary tumor samples from different mice. Variation in patterns of gene expression was seen, with ~75% of outlier genes found to be common in replicate experiments. Thirty-one genes common to replicate experiments were overexpressed in K7M2 compared with K12 primary tumors, and 22 genes were overexpressed in K12 compared with K7M2 primary tumors (Tables 1 and 2).

Microarray Outlier Classification. To better understand the potential importance of each outlier gene and to define genes most likely to be associated with differences in the metastatic biology of the models, each outlier gene was assigned to two classification systems. The first classification, using a modification of the National Center for Biotechnology Information Clusters of Orthologous Gene Classification,[4] was based on the basic function of each gene. Assignment of a gene to a basic function classification group was mutually exclusive (Tables 1 and 2). The second classification of each gene was to six nonmutually exclusive metastasis-associated processes (proliferation/apoptosis, motility/cytoskeleton, invasion, adhesion, immune surveillance, and angiogenesis). The assignment of each gene into both classification systems is presented in Tables 1 and 2. Twenty-nine of the 53 differentially expressed genes could be categorized into metastasis-related functions. Northern analysis confirmed the pattern of differential gene expression identified by cDNA microarray for selected genes (Fig. 2).

Using the information in Tables 1 and 2, we returned to the K7M2 and K12 models to uncover specific differences in their biologies for each of the six metastasis-associated processes (proliferation/apoptosis, motility/cytoskeleton, invasion, adhesion, immune surveillance, and angiogenesis). The six metastasis-associated processes examined were considered to be important steps in the cascade of events that follows a tumor cell from its primary site to a distant metastatic site. The metastasis-associated processes of proliferation/apoptosis and angiogenesis were examined in the original report of the K7M2/K12 model (2). These studies demonstrated no difference in apoptosis or proliferation between K7M2 and K12 but did demonstrate significant differences in tumor angiogenesis favoring K7M2.

Motility and Cytoskeleton. To define differences in the cytoskeleton of the OSA cells, we examined their F-actin cytostructural architecture. Significant differences in the size and morphology of the K7M2 and K12 cells was demonstrated by F-actin staining (Fig. 3). The K7M2 cells were larger, had more numerous cellular extensions (filapodia and pseudopodia), greater substrate contact points, and enhanced spread phenotype than the K12 cells. Cellular extensions were less common and were significantly shorter in the K12 compared with the K7M2 cells. K12 cells contained organized actin stress filaments in the body of the cells, whereas in K7M2 actin stress filaments were concentrated within cellular extensions. In K7M2 cells, cytoplasmic actin was primarily punctate with very little in polymerized forms. Foot processes from cellular extensions in the K7M2 cells had very high levels of F-actin. Actin-rich fragments, not associated with the cells, were common in preparations of the K7M2
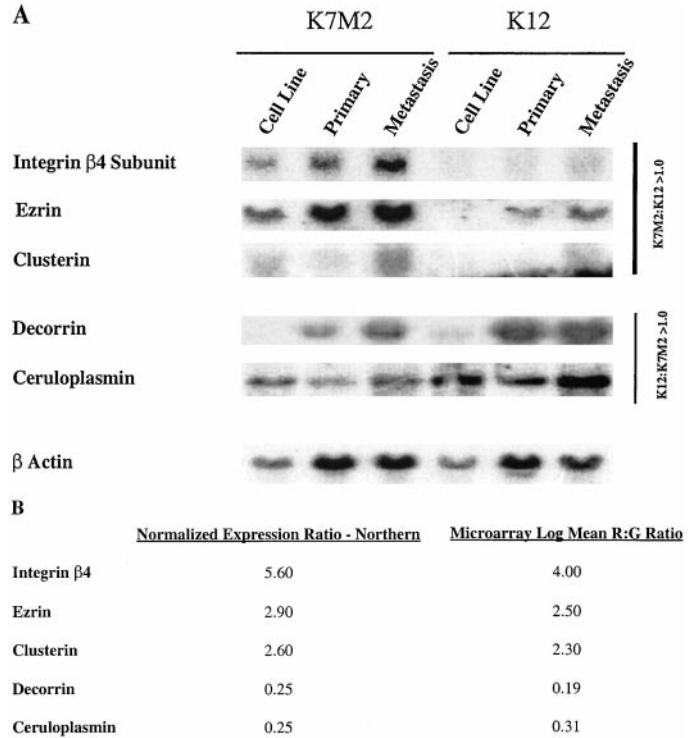
Fig. 2. Analysis of differential gene expression in K7M2 and K12 using Northern analysis. *A*, Northern analysis of selected genes (*Integrin β4 Subunit, Ezrin, Clusterin, Decorrin,* and *Ceruloplasmin*) found differentially expressed between K7M2 and K12 tissues by microarray. *Lane 1*, K7M2 cell culture RNA; *Lane 2*, K7M2 primary tumor RNA; *Lane 3*, K7M2 pulmonary metastasis RNA; *Lane 4*, K12 cell culture RNA; *Lane 5*, K12 primary tumor RNA; *Lane 6*, K12 pulmonary metastasis RNA. For genes overexpressed in the more aggressive K7M2 *versus* K12 (*Integrin β4 subunit, Ezrin,* and *Clusterin*), there was a higher level of gene expression in RNA from pulmonary metastases compared with primary tumor and cell culture RNA. Equal loading of 25 μg of total RNA was demonstrated by hybridization of representative Northern blot with a murine β-actin cDNA probe. *B*, concordance of differential gene expression of K7M2 *versus* K12 primary tumor using cDNA microarray and Northern. The log mean *red:green* (*R:G*) ratio defined by microarray (Tables 1 and 2) is compared with a Northern densitometric quantification (standardized against the β-actin signal).

cell line and absent from the K12 cells. These cell-free fragments demonstrated similar patterns of actin expression as the K7M2 foot processes. F-actin staining seemed to suggest a greater potential for motility in the K7M2 compared with the K12 cells. To examine this potential difference in cellular motility, we performed *in vitro* motility experiments using Transwell tissue culture plates. In these assays, motility was defined as migration of cells from the apical surface of the Transwell membrane through 8-μm pores to the basal surface of the membrane. Significantly greater *in vitro* motility was demonstrated in the K7M2 cells compared with the K12 cells for all time points evaluated (4, 12, 24, 48, and 72 h of culture; *P* < 0.001; Fig. 4). The number of cells leaving the basal surface of the Transwell membrane into the lower chamber was small (<2% of plated cells) and was similar for K7M2 and K12 cell lines (data not shown).

Invasion. The invasion phenotype of K7M2 and K12 cells was assessed by comparing their relative abilities to invade tumor extracellular matrix (Matrigel) using the Transwell culture system described above. Both cells were invasive through Matrigel; however, no differences in invasion could be demonstrated between K7M2 and K12 cell lines at any time points examined (data not shown). To further examine the invasion phenotype of the OSA cells, MMP activity was assessed using gelatinase zymography. MMP-2 and MMP-9 activity was detected in both K7M2 and K12 cell line supernatant and cellular pellets. No significant differences in the precursor or active forms for MMP-2 or MMP-9 were demonstrable between K7M2 and K12 (data not shown).
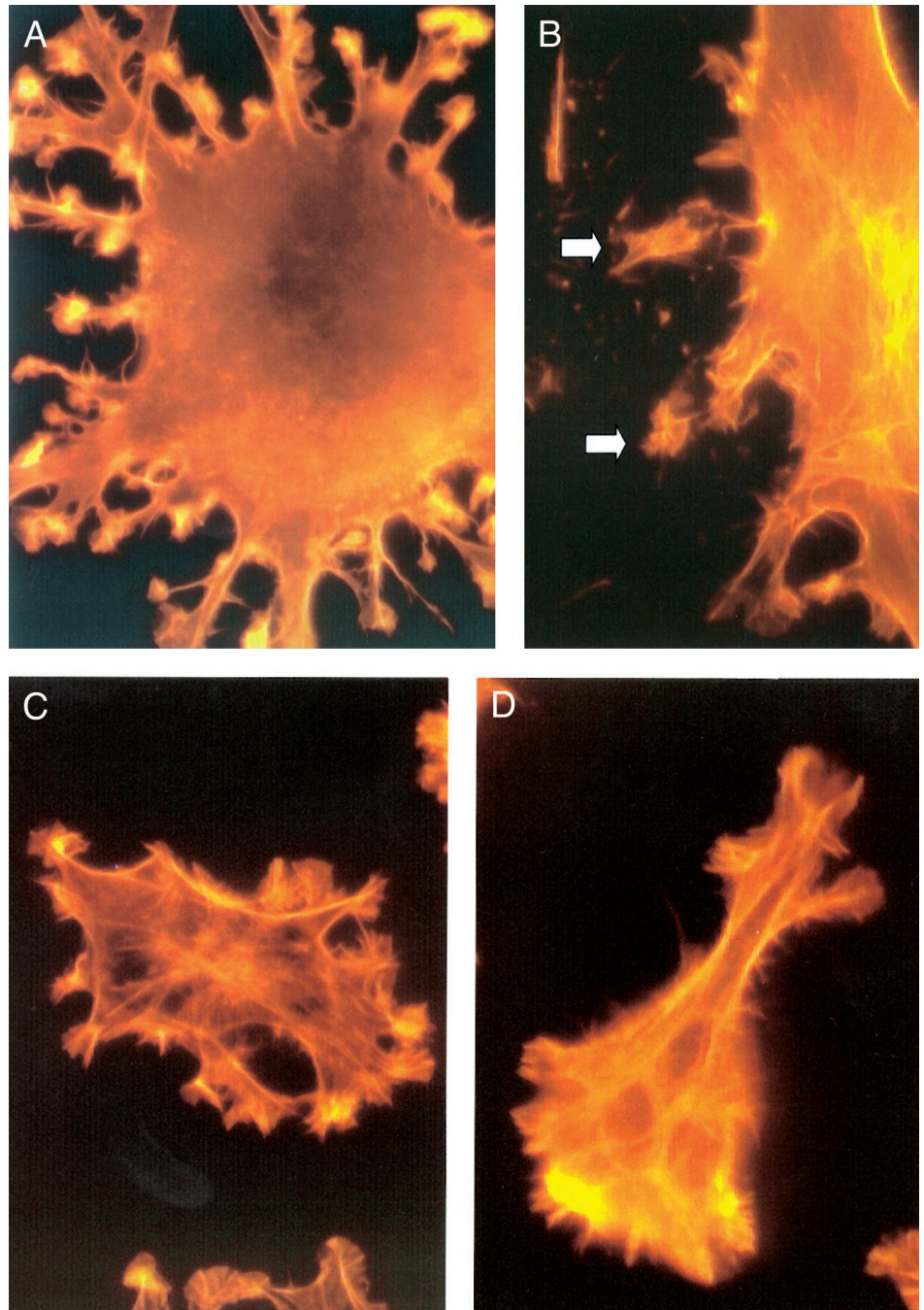
Fig. 3. Rhodamine phalloidin staining for F-actin in K7M2 and K12 cells revealed significant differences in cellular size and morphology. *A* and *B*, K7M2 cells were larger cells (with greater cell-to-cell differences in size) with many cellular extensions (filapodia and pseudopodia) and actin-rich foot processes (×630). In K7M2, actin was primarily punctate and depolymerized. *B*, cell-free fragments, with high levels of actin, were seen frequently in the K7M2 cells and were absent from the K12 cells (*white arrow*). *C* and *D*, K12 cells were smaller with less frequent and shorter cellular extensions (×630). Actin stress fibers were common in the K12 cells.

Heterotypic Adhesion. Differences in the heterotypic adherence (cell-to-substrate adherence) of K7M2 and K12 cells were examined using type IV collagen and Matrigel as substrates. Adherence was assessed at early (0.5 and 1.5 h) and late time points (12, 24, and 48 h). The ability to initiate early adherence has been described as a distinct process from the maintenance of adhesion by cancer cells. Heterotypic adherence to both type IV collagen and Matrigel was significantly greater in K7M2 cells compared with K12 cells after 0.5 and 1.5 h of culture (early adherence; $P < 0.01$; Fig. 5). However, no significant difference in heterotypic adhesion was observed between K7M2 and K12 cells for the late adherence (maintenance of adherence) time points for either type IV collagen or Matrigel. Heterotypic adhesion for both K7M2 and K12 increased significantly from 12 to 24 to 48 h ($P < 0.01$). Microscopic evaluation of 96-well plates suggested that homotypic adhesion

(cell-to-cell adhesion) may have contributed to the total adhesion measured at time points after 48 h.

Immune Surveillance. Given that the K7M2 and K12 cells were clonally derived and selected *in vivo*, it is possible that minor histocompatibility differences could develop between the two clones. These "differences" may be recognition determinants for the immune system of the syngeneic (immune-competent) BALB/c hosts. Greater immune recognition and elimination of the K12 cells may explain the less aggressive behavior of the K12 model. To address this possibility an experimental metastasis assay (tail vein injection) using K7M2 and K12 cells was undertaken in completely immunocompromised (scid-beige) mice. The more aggressive phenotype of the K7M2 cells was maintained even in scid-beige mice. Death from experimental metastasis occurred after tail vein injection of K7M2 cells at 15 ± 3 days (median $\pm$ SD) compared with 76 ± 21 days in mice injected with
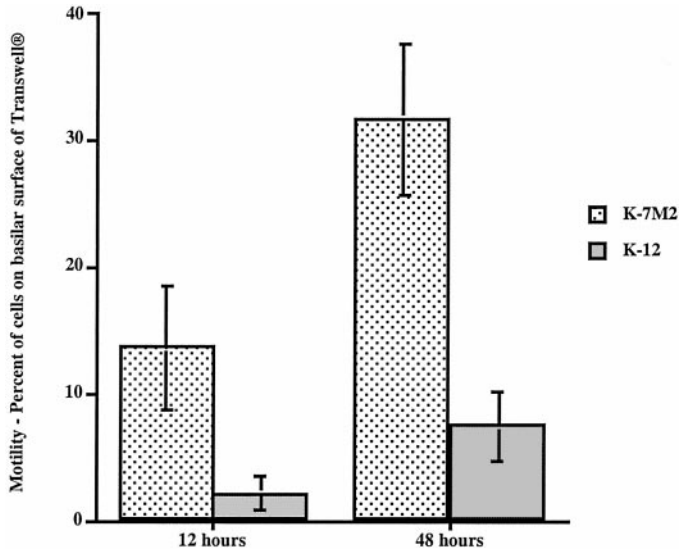
Fig. 4. *In vitro* motility, assessed using Transwell culture plates, was significantly greater in K7M2 compared with K12 cell lines at 4, 12, 24, 48, and 72 h (∗, *P* < 0.001; data for 4, 24, and 72 h not shown). The percentage of motility was the proportion of cells passing from the top chamber of the Transwell to the bottom surface of the Transwell membrane. Staining of the Transwell membrane with DiffQuick allowed microscopic enumeration of cells. *Bars,* SD.

K12 (*P* < 0.001). The lung was the only site of metastasis seen after tail vein injection of either cell line.

On the basis of the studies comparing the K7M2 and K12 model for each of six metastasis-associated processes, we concluded that differences in motility/cytoskeleton, heterotypic adherence, and angiogenesis (tumor vascularity, as assessed in the original report of the model; Ref. 2) were most likely to explain the more aggressive behavior of the K7M2 compared with the K12 models. For this reason, special attention was directed to the microarray outliers that had been assigned to the motility/cytoskeleton, heterotypic adherence, and angiogenesis categories (Tables 1 and 2). The 10 microarray outliers (taken from Tables 1 and 2) assigned to these three metastasis-associated categories are presented in Table 3. *Ezrin,* a gene not described previously in mesenchymal tumors, was examined further based on its described functions in several metastasis-associated processes and its novelty to OSA.

Ezrin. To verify the differential expression of ezrin at the protein level, we performed *in situ* immunostaining using ezrin antibodies in K7M2 and K12 cells. Immunocytological staining for ezrin detected a stronger signal in K7M2 cells compared with K12 cells (Fig. 6). The strongest ezrin staining signal was seen at the cytoplasmic boundaries, cellular extensions, and foot processes of the K7M2 cells. The absence of ezrin staining in the K12 cellular extensions was notable. This pattern of ezrin staining was similar to the distribution of F-actin seen in K7M2 cells (Fig. 3). The potential relevance of ezrin in human OSA was assessed by Northern analysis of human OSA cell lines. High expression of ezrin was found in four of five human OSA cell lines (Fig. 7). Ezrin expression in the fifth cell line, G292, was low but specific for ezrin in repeat Northern hybridizations.

DISCUSSION

The well-defined differences in metastatic behavior and the clonal relationship of the K7M2 and K12 cells allowed the use of cDNA microarrays to define potentially important genetic determinants for pulmonary metastasis in this model. Recently, cDNA microarray technology has been used to list genes that are differentially expressed between high and low metastatic tumor systems (18–20). Data gen-

erated in such cDNA microarray comparisons are of considerable value; however, it is difficult to determine how best to use this information. Both traditional reductionist and novel bio-informatic approaches (including hierarchical cluster analyses) have been used to manage microarray data. In the cDNA microarray comparisons presented herein, we identified 53 genes that were differentially expressed between the high (K7M2) and the low (K12) metastatic OSA primary tumors. To use this information, we used a reductionist approach that was based on biological differences demonstrated between the high and low metastatic models for six metastasis-related processes. Each of the 53 differentially expressed genes was assigned to nonmutually exclusive metastasis-related process categories using the gene name and the terms "cancer," "metastasis," "proliferation," "apoptosis," "motility," "cytoskeleton," "invasion," "immune," "adherence," and "angiogenesis" in a PubMed search of the literature. Then studies were designed to compare K7M2 and K12 for functional differences in each of these six metastasis-associated processes. The rationale for this approach was that if a significant difference in a metastasis-related process (*e.g.,* motility and cytoskeleton) was defined between K7M2 and K12, then the genes assigned to that process (from the literature) would be more likely to explain the differences in pulmonary metastatic behavior of the models. Conversely, if no difference in a metastasis-related process (*e.g.,* proliferation/apoptosis) was defined between K7M2 and K12, then genes assigned to that process would be less likely to explain the differences. This functional approach was not meant to exclude genes from consideration rather to focus attention on those genes most likely to be associated with
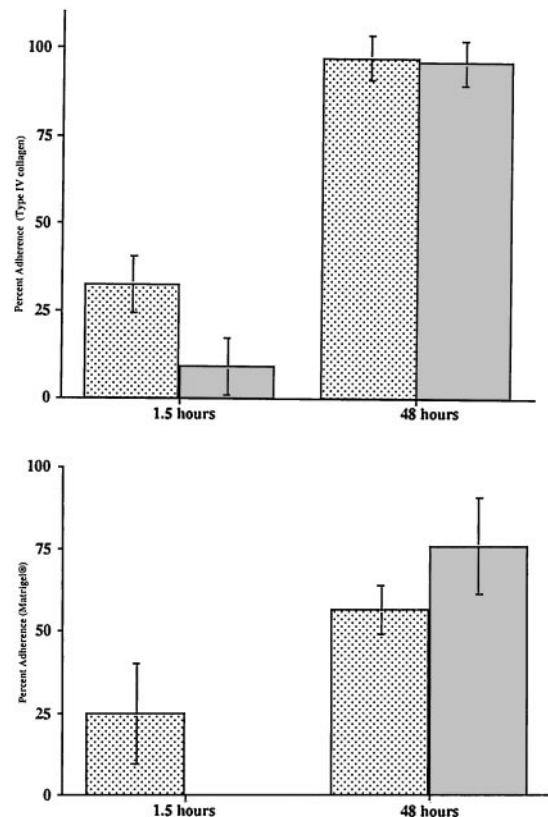
Fig. 5. Heterotypic adherence assay using type IV collagen (*A*) and Matrigel substrates (*B*) demonstrated increased "early" adherence for K7M2 compared with K12 at 0.5 and 1.5 h of culture (*P* < 0.01; data not shown at 0.5 h). No differences in adherence "maintenance" between K7M2 and K12 cell lines were noted after 24 and 48 h of culture (data not shown for 24 h). The percentage of adherence was the proportion of cells plated that remain adherent to the respective substrates after a defined plate wash. Representative data are presented (experimental conditions repeated in quadruplicate; assays repeated four times). ▨, K7M2; ■, K12. *Bars,* SD.

Table 3 *Narrowed pool of microarray (cDNA) outliers associated with motility/cytoskeleton, heterotypic adherence, or angiogenesis*

Gene name[a]	Metastasis-associated process[b]
Integrin β4	Motility/cytoskeleton; adherence
Connective tissue growth factor	Angiogenesis
Integrin αV	Motility/cytoskeleton; adherence; angiogenesis
Ezrin	Motility/cytoskeleton; adherence; angiogenesis
Integrin β2	Adherence
Galectin-3	Motility/cytoskeleton; adherence; angiogenesis
A disintegrin and metalloprotease domain (ADAM) 8	Motility/cytoskeleton; adherence
Clusterin	Adherence
FARP1	Motility/cytoskeleton; adherence
Ceruloplasmin	Angiogenesis

[a] Genes found differentially expressed and associated with metastasis-associated processes of motility/cytoskeleton, heterotypic adherence, and/or angiogenesis.

[b] Association with processes of motility/cytoskeleton, adherence, or angiogenesis.

differences in pulmonary metastasis in the model. Functional studies for the metastasis-associated processes demonstrated significant differences in motility and cytoskeleton, heterotypic adherence, and angiogenesis in K7M2 compared with K12. No differences in proliferation and apoptosis, invasion, or immune detection, which would favor K7M2 tumor growth or metastasis over K12, were seen. For these reasons, the 10 genes defined by cDNA microarray that were assigned to the motility and cytoskeleton, heterotypic adherence, and angiogenesis categories were most likely to be associated with differences in K7M2 and K12 metastatic behavior. This narrowed pool of 10 genes (Table 3) is the result of microarray analysis, assignment of genes to metastasis processes, and detailed functional studies that compared the K7M2 and K12 models in each of these six metastasis-associated processes.

The outlier genes identified in the comparison of K7M2 and K12 tumors included several that have not been described previously in OSA (*e.g., galectin-3, ezrin,* and *clusterin*). This is to be expected and is an advantage of a cDNA microarray that included a wide variety of genes. Microarrays that only include genes from a specific field (*i.e.,* OSA or cancer) would not share this advantage. It is not surprising that >50% of known genes (excluding ESTs with no known functions) identified in this analysis were placed into at least one metastasis-related category. This high rate of assignment of genes is related to the design of the experiments (use of clonally related models differing in spontaneous pulmonary metastatic potential) and the bias of the method (PubMed literature search) by which genes were assigned to categories. Another important feature of the arrays used herein is the inclusion of ESTs. Their inclusion has allowed three ESTs, not currently in a UniGene cluster, to be associated with the metastatic behavior observed in the model system. A common concern with data generated by cDNA microarray analysis is the validation of the gene outlier list. We have reported previously on the high
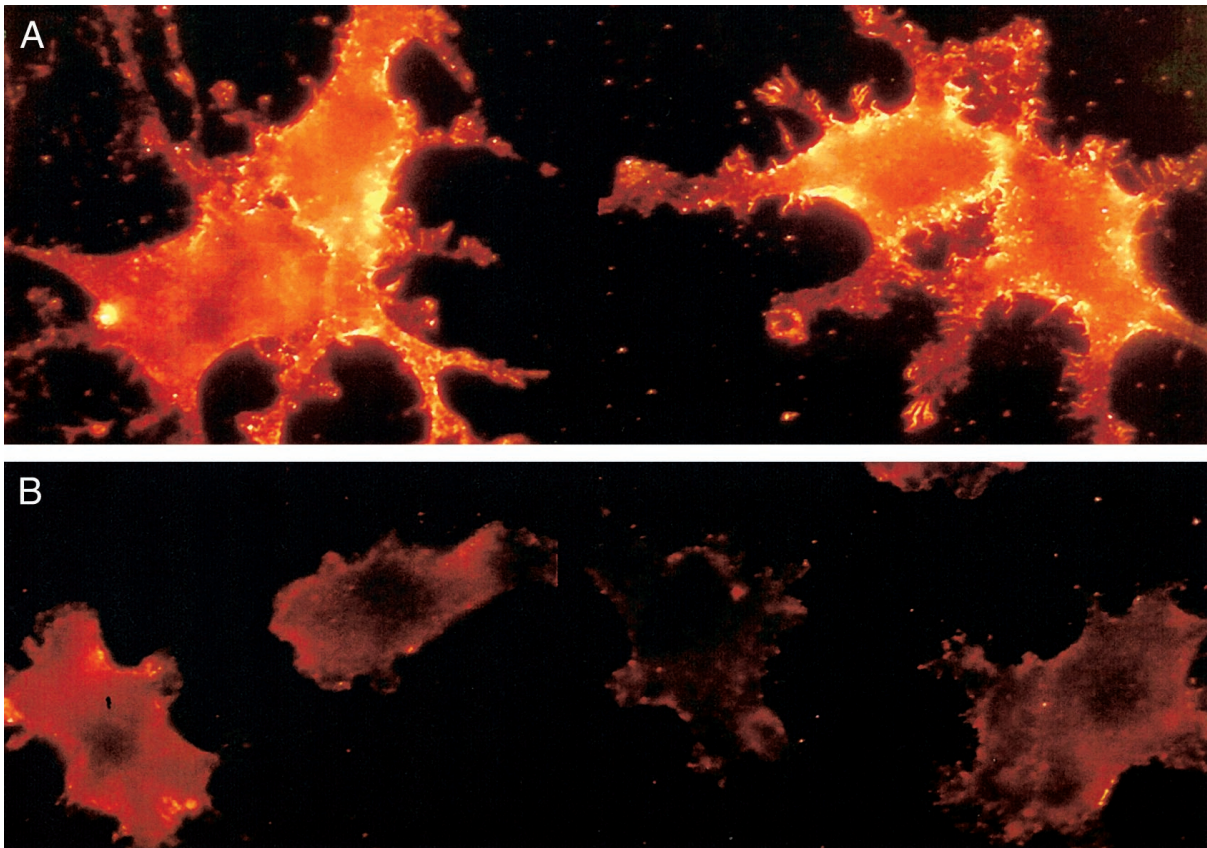
Fig. 6. Increased ezrin protein is demonstrated in immunocytological coverslip preparations of K7M2 compared with K12. *A,* ezrin staining is diffuse in the cytoplasm of K7M2 with enhanced staining at cytoplasmic boundaries, along cellular extensions, and at cellular extension foot processes. *B,* decreased staining for ezrin is present in K12 cells. Very little accumulation of ezrin is noted at cell membranes or at cellular processes. Negative control staining with the ezrin polyclonal antibody alone or Cy3 secondary antibody alone revealed little nonspecific staining (data not shown).
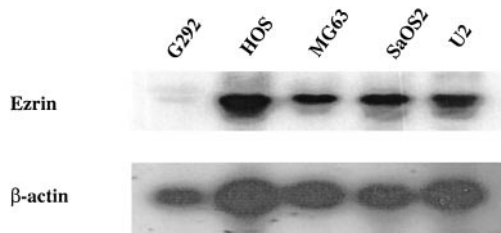
Fig. 7. Ezrin is expressed in five of five human OSA cell lines. Northern analysis of human OSA cell lines (G292, HOS, MG63, SaOS2, and U2) demonstrates high levels of ezrin expression for all cell lines except G292. Ezrin expression in G292 was low but specific for ezrin in repeated Northern hybridizations.

concordance of gene expression defined by our cDNA microarray and Northern analysis (11). This concordance was confirmed by Northern for a selected number of genes defined in our study and was further validated at the protein level, using immunostaining, for ezrin.

The importance of motility during metastasis has been reviewed recently (21–24). *In vitro* motility assays and differences in actin cytoskeleton staining strongly supported the enhanced motility phenotype of K7M2 compared with K12. The presence of cellular extensions, including filapodia and lamellipodia, have been associated previously with tumor motility, invasiveness, and metastasis in several tumor models and supports the more aggressive (motility) phenotype of the K7M2 cells. K7M2 cells appear to be "primed" for motility, with little polymerized cytoplasmic F-actin, awaiting environmental cues with stress filaments organized at the periphery of the cell. Support for this hypothesis comes from studies of motile renal epithelial cells that demonstrate increased motility and decreased F-actin stress cable formation after stimulation of the hepatocyte-growth factor pathway (25). The presence of actin-rich fragments, found free from the K7M2 cells, may also support enhanced motility. These fragments may represent a passive fracture of cytoplasmic foot processes seen in highly motile cells. It is also possible that they represent an active process of cytoplasmic shedding associated with tumor stroma formation.

Differences in the motility of K7M2 and K12 cells focused our attention on the cDNA microarray outliers (genes) associated with motility. Interesting members of the motility category include *ezrin* and *galectin-3*. Neither of these genes have been reported previously in OSA. Ezrin is a member of the ERM and merlin family of genes (26). The protein products of the *ERM* genes are part of the band 4.1 protein superfamily (27). Ezrin is a downstream effector of the Rho kinase signaling pathway, acting as a cytoplasmic linker of F-actin with the cell membrane (28). The importance of the RhoC and the Rho/Rho kinase signaling pathway in cell motility, actin cytoskeleton, and metastasis has been demonstrated recently (20). The parallel distribution of F-actin and ezrin protein at cytoplasmic boundaries, within cellular extensions, and at foot processes suggests the role of ezrin in the motility and actin cytostructure of K7M2 cells. The immunocytostaining and distribution of ezrin in the K7M2 cells lend support for the biological role of ezrin in the more aggressive K7M2 cells. The potential importance of ezrin in human OSA was supported by high expression in four of five and detectable levels in five of five human OSA cell lines. This is the first report of *ezrin* expression in OSA, a gene more commonly associated with epithelial tissues. Further work should examine the role of ezrin in other mesenchymal tissues and malignancies.

The ability of a cancer cells to adhere to substrates at distant sites (*i.e.,* the pulmonary arterioles and venules) is essential for successful metastasis. The importance and timing of heterotypic adhesion in this process are currently under debate (29–31). Using a simple *in vitro* assay of heterotypic adherence, the increased ability of the K7M2

cells to adhere to type IV collagen and Matrigel at 0.5 and 1.5 h of culture (suggestive of enhanced early heterotypic adhesion) was demonstrated. No differences in heterotypic adhesion were seen after culture periods of 12 h, suggesting equivalent abilities of the K7M2 and K12 cells to maintain adherence. After longer culture times, it is possible that homotypic (cell-to-cell) adhesion contributed to the total adhesion measured in the *in vitro* assay. Interestingly, the ERM family of genes (including *ezrin*) have been associated with early heterotypic adherence and not necessarily associated with the ability to maintain late adherence (30). Another gene with adherence-associated functions is *galectin-3*. Galectin-3 is a lectin binding protein that has been associated previously with a malignant phenotype in several epithelial cancers including prostate and colon carcinomas (32, 33). Galectin-3 may be also associated with metastasis through its demonstrated roles in tumor motility and invasion (34). The diverse metastasis-associated functions of galectin-3, including heterotypic adherence, make it an interesting candidate for evaluation in sarcomas including OSA.

In our previous characterization of the K7M2 and K12 models, enhanced angiogenesis of the K7M2 model was documented by CD31 and factor VIII staining of the primary tumor and the pulmonary metastases (2). The presence of ill-formed vascular structures, which interacted with nearly all tumor cells, was evident in sections of the K7M2 primary tumor and pulmonary metastasis. Conversely, the K12 tumor cells were densely packed with very few vascular structures present. In this earlier work, expression patterns for several angiogenesis-associated genes, including *flt1, flt4, TIE1, TIE2, CD31,* and *VEG-F,* were similar in cell lines, primary tumors, and metastases from both K7M2 and K12 models. The strong difference in the angiogenic phenotype of the models and the lack of differences in gene expression for the "classical" angiogenesis-associated genes suggest the possibility that a less well-recognized angiogenesis-associated gene, potentially defined by our microarray analysis [*connective tissue growth factor, integrin αV (CD51),* or *galectin-3*], may be important in defining the angiogenic phenotype of the more aggressive K7M2 model.

On the basis of our functional characterization of the K7M2 and K12 cell lines and tissues, genes associated with proliferation and apoptosis, tumor invasion, and immune surveillance were considered to be less important determinants of metastasis in this model. This is not to say that these processes are not important for metastasis; rather, that these processes are less likely to characterize the differences in metastases observed between K7M2 and K12. Defining the importance of genes using this functional approach depends on valid and relevant assays for each metastasis-related process. It is also dependent on the correct assignment of a gene within a functional group (using PubMed database searches). The proliferation and apoptotic rate of the tumor models was assessed *in vitro* (doubling time) and *in vivo* (immunohistochemical staining with Ki67 and terminal deoxynucleotidyltransferase-mediated nick end labeling) in our initial characterization of the model (2). The concordance of findings in both *in vitro* and *in vivo* assays suggested that differences in resting proliferation and apoptosis rates do not provide a metastatic advantage for K7M2. Tumor invasion was assessed using a simple Matrigel invasion assay and by measuring MMP activities in K7M2 and K12 cells. Similar assays have been used to assess the invasive potential of tumor cells (35). Both assays failed to demonstrate significant differences in the invasive phenotype of K7M2 and K12. The sensitivity of the Matrigel invasion assay may be low and may not have detected subtle differences in the invasive phenotype of the K7M2 and K12 cells. An *in vivo* system was used to examine whether differences in immune surveillance could account for differences in the biology of K7M2 and K12. It is possible that minor histocompatibility differences could emerge in two clonally related cell lines and that these

differences could result in the more effective immune recognition and destruction of one tumor cell line compared with another. Our results demonstrate that the relative metastatic phenotype of the K7M2 and K12 cell lines was maintained in significantly immunocompromised animals (beige-scid mice). Therefore, genes associated with the immune surveillance and immune rejection of cancer are less likely to characterize the differences in the biology of K7M2 and K12.

Using a well-characterized murine model, a microarray that includes a large and diverse number of cDNA probes, and a functional approach to analyze microarray outliers, we have defined several potentially important genes associated with pulmonary metastasis in OSA. Genes identified in this work include those not described previously in OSA as well as potentially novel metastasis-associated genes (ESTs). Functional studies suggest that 10 genes associated with motility/cytoskeleton, heterotypic adherence, and angiogenesis are most likely to be associated with differences in the metastatic behavior of the high and low metastatic OSA model. Genes identified in this analysis may have relevance to OSA and other solid tumors with high rates of pulmonary metastasis. A motility, adherence, and invasion gene called *ezrin* was identified using this approach. The differential expression of ezrin protein was confirmed in K7M2 and K12 cells and the potential relevance of ezrin in human OSA suggested by finding its expression in five of five human OSA cell lines. This work represents a rationale approach to the evaluation of microarray data and will be useful to identify genes that may be causally associated with metastasis.

REFERENCES

1. Bruland, O. S., and Pihl, A. On the current management of osteosarcoma. A critical evaluation and a proposal for a modified treatment strategy. Eur. J. Cancer, *33:* 1725–1731, 1997.
2. Khanna, C., Prehn, J., Yeung, C., Caylor, J., Tsokos, M., and Helman, L. An orthotopic murine model of osteosarcoma with clonally related variants differing in pulmonary metastatic potential. Clin. Exp. Metastasis, *18:* 261–271, 2001.
3. Schmidt, J., Straub, G. P., Schon, A., Luz, A., Murray, B., Melchiori, A., Aresu, O., and Erfle, V. Establishment and characterization of osteogenic cell lines from a spontaneous murine osteosarcoma. Differentiation, *39:* 151–160, 1988.
4. Lam, A. K. Molecular biology of esophageal squamous cell carcinoma. Crit. Rev. Oncol. Hematol., *33:* 71–90, 2000.
5. Portera, C. A., Berman, R. S., and Ellis, L. M. Molecular determinants of colon cancer metastasis. Surg. Oncol., *7:* 183–195, 1998.
6. Bangma, C. H., Nasu, Y., Ren, C., and Thompson, T. C. Metastasis-related genes in prostate cancer. Semin. Oncol., *26:* 422–427, 1999.
7. Woodhouse, E. C., Chuaqui, R. F., and Liotta, L. A. General mechanisms of metastasis. Cancer (Phila.), *80:* 1529–1537, 1997.
8. Lamb, R. F., Ozanne, B. W., Roy, C., McGarry, L., Stipp, C., Mangeat, P., and Jay, D. G. Essential functions of ezrin in maintenance of cell shape and lamellipodial extension in normal and transformed fibroblasts. Curr. Biol., *9:* 682–688, 1997.
9. Ohtani, K., Sakamoto, H., Rutherford, T., Chen, Z., Satoh, K., and Naftolin, F. Ezrin, a membrane-cytoskeletal linking protein, is involved in the process of invasion of endometrial cancer cells. Cancer Lett., *147:* 31–38, 1999.
10. Gerstenfeld, L. C., Uporova, T., Schmidt, P. G., Straus, P. G., Shih, S. D., Huang, L. F., Gundberg, C., Mizuno, S., and Glowacki, J. Osteogenic potential of murine osteosarcoma cells: comparison of bone-specific gene expression *in vitro* and *in vivo* conditions. Lab. Investig., *74:* 895–906, 1996.
11. Khan, J., Bittner, M. L., Saal, L. H., Teichmann, U., Azorsa, D. O., Gooden, G. C., Pavan, W. J., Trent, J. M., and Meltzer, P. S. cDNA microarrays detect activation of a myogenic transcription program by the PAX3-FKHR fusion oncogene. Proc. Natl. Acad. Sci. USA, *96:* 13264–13269, 1999.
12. Khan, J., Simon, R., Bittner, M., Chen, Y., Leighton, S. B., Pohida, T., Smith, P. D., Jiang, Y., Gooden, G. C., Trent, J. M., and Meltzer, P. S. Gene expression profiling of alveolar rhabdomyosarcoma with cDNA microarrays. Cancer Res., *58:* 5009–5013, 1998.
13. Chen, Y., Dougherty, E. R., and Bittner, M. L. Ratio-based decisions and the quantitative analysis of cDNA microarray images. Biomedical Optics, *2:* 364–374, 1997.
14. Lana, S. E., Ogilvie, G. K., Hansen, R. A., Powers, B. E., Dernell, W. S., and Withrow, S. J. Identification of matrix metalloproteinases in canine neoplastic tissue. Am. J. Vet. Res., *61:* 111–114, 2000.
15. Eliopoulos, A. G., Kerr, D. J., Herod, J., Hodgkins, L., Krajewski, S., Reed, J. C., and Young, L. S. The control of apoptosis and drug resistance in ovarian cancer: influence of p53 and bcl-2. Oncogene, *11:* 1217–1228, 1995.
16. Anderson, P. M., Katsanis, E., Leonard, A. S., Schow, D., Loeffler, C. M., Goldstein, M. B., and Ochoa, A. C. Increased local antitumor effects of interleukin-2 liposomes in mice with MCA-106 sarcoma pulmonary metastases. Cancer Res., *50:* 1853–1856, 1990.
17. N. A. R. A. (Committee) Using Animals in Intramural Research. Guidelines for Investigators and Guidelines for Animal Users. Bethesda, MD: NIH, 1998.
18. Bittner, M., Meltzer, P., Chen, Y., Jiang, Y., Seftor, E., Hendrix, M., Radmacher, M., Simon, R., Yakhini, Z., Ben-Dor, A., Sampas, N., Dougherty, E., Wang, E., Marincola, F., Gooden, C., Lueders, J., Glatfelter, A., Pollock, P., Carpten, J., Gillanders, E., Leja, D., Dietrich, K., Beaudry, C., Berens, M., Alberts, D., Sondak, V., Hayward, N., and Trent, J. Molecular classification of cutaneous malignant melanoma by gene expression profiling. Nature (Lond.), *406:* 536–540, 2000.
19. Maniotis, A. J., Folberg, R., Hess, A., Seftor, E. A., Gardner, L. M., Pe'er, J., Trent, J. M., Meltzer, P. S., and Hendrix, M. J. Vascular channel formation by human melanoma cells *in vivo* and *in vitro*: vasculogenic mimicry. Am. J. Pathol., *155:* 739–752, 1999.
20. Clark, E. A., Golub, T. R., Lander, E. S., and Hynes, R. O. Genomic analysis of metastasis reveals an essential role for RhoC. Nature (Lond.), *406:* 532–535, 2000.
21. Banyard, J., and Zetter, B. R. The role of cell motility in prostate cancer. Cancer Metastasis Rev., *17:* 449–458, 1999.
22. Mahadevan, L., and Matsudaira, P. Motility powered by supramolecular springs and ratchets. Science (Wash. DC), *288:* 95–100, 2000.
23. Machesky, L. M., and Hall, A. Role of actin polymerization and adhesion to extracellular matrix in Rac- and Rho-induced cytoskeletal reorganization. J. Cell Biol., *138:* 913–926, 1997.
24. Borisy, G. G., and Svitkina, T. M. Actin machinery: pushing the envelope. Curr. Opin. Cell Biol., *12:* 104–112, 2000.
25. Crepaldi, T., Gautreau, A., Comoglio, P. M., Louvard, D., and Arpin, M. Ezrin is an effector of hepatocyte growth factor-mediated migration and morphogenesis in epithelial cells. J. Cell Biol., *138:* 423–434, 1997.
26. Vaheri, A., Carpen, O., Heiska, L., Helander, T. S., Jaaskelainen, J., Majander-Nordenswan, P., Sainio, M., Timonen, T., and Turunen, O. The ezrin protein family: membrane-cytoskeleton interactions and disease associations. Curr. Opin. Cell Biol., *9:* 659–666, 1997.
27. Mangeat, P., Roy, C., and Martin, M. ERM proteins in cell adhesion and membrane dynamics. Trends Cell Biol., *9:* 187–192, 1999.
28. Gautreau, A., Louvard, D., and Arpin, M. Morphogenic effects of ezrin require a phosphorylation-induced transition from oligomers to monomers at the plasma membrane. J. Cell Biol., *150:* 193–203, 2000.
29. Luca, M., Hunt, B., Bucana, C. D., Johnson, J. P., Fidler, I. J., and Bar-Eli, M. Direct correlation between MUC18 expression and metastatic potential of human melanoma cells. Melanoma Res., *3:* 35–41, 1993.
30. Gronholm, M., Sainio, M., Zhao, F., Heiska, L., Vaheri, A., and Carpen, O. Homotypic and heterotypic interaction of the neurofibromatosis 2 tumor suppressor protein merlin and the ERM protein ezrin. J. Cell Sci., *112:* 895–904, 1999.
31. Chambers, A. F., MacDonald, I. C., Schmidt, E. E., Koop, S., Morris, V. L., Khokha, R., and Groom, A. C. Steps in tumor metastasis: new concepts from intravital videomicroscopy. Cancer Metastasis Rev., *14:* 279–301, 1995.
32. Perillo, N. L., Marcus, M. E., and Baum, L. G. Galectins: versatile modulators of cell adhesion, cell proliferation, and cell death. J. Mol. Med., *76:* 402–412, 1998.
33. Nakamura, M., Inufusa, H., Adachi, T., Aga, M., Kurimoto, M., Nakatani, Y., Wakano, T., Nakajima, A., Hida, J. I., Miyake, M., Shindo, K., and Yasutomi, M. Involvement of galectin-3 expression in colorectal cancer progression and metastasis. Int. J. Oncol., *15:* 143–148, 1999.
34. Bresalier, R. S., Mazurek, N, Sternberg, L. R., Byrd, J. C., Yunker, C. K., Nagia-Makker, P., Raz, A. Metastasis of human color cancer is altered by modifying expression of beta-galactoside binding protein. Gastroenterology, *115:* 287–297, 1998.
35. Bjornland, K., Winberg, J. O., Odegaard, O. T., Hovig, E., Loennechen, T., Aasen, A. O., Fodstad, O., and Maelandsmo, G. M. S100A4 involvement in metastasis: deregulation of matrix metalloproteinases and tissue inhibitors of matrix metalloproteinases in osteosarcoma cells transfected with an anti-S100A4 ribozyme. Cancer Res., *59:* 4702–4708, 1999.